Penerbit Akademia Baru

CFD Letters

Journal homepage: www.akademiabaru.com/cfdl.html
ISSN: 2180-1363

Temperature Minimization on the Substrate of a Heat Sink By Rib-Groove Microchannel Heat Sink with Effective Energy Consumption: Groove Geometry Parameter Effects

Open Access

Wan Mohd. Arif Aziz Japar[1], Nor Azwadi Che Sidik[1,*], R. Saidur[2], Yutaka Asako[1], Mohd Irwan Mohd Azmi[1]

[1] Malaysia – Japan International Institute of Technology (MJIIT), Universiti Teknologi Malaysia Kuala Lumpur, Jalan Sultan Yahya Petra, 54100 Kuala Lumpur, Malaysia
[2] Research Centre for Nano-Materials and Energy Technology, School of Science and Technology, Sunway University, Bandar Sunway, 47500 Subang Jaya, Selangor, Malaysia

ARTICLE INFO

Article history:
Received 20 July 2019
Received in revised form 15 September 2019
Accepted 20 September 2019
Available online 28 September 2019

ABSTRACT

With the unpredicted increment of power density in Microelectromechanical systems (MEMS) device, an effective cooling technique like micro-cooling method is required to ensure temperature of the device not exceeds or near to the allowable temperature for semiconductor component (Allowable temperature < 358.15 K). Microchannel heat sink is one of the best candidate among micro-cooling method which can meet a cooling demand for current electronic devices. The temperature of a substrate of microchannel heat sink is very important because the substrate directly attaches to the electronic components. By increasing a mass flowrate in a conventional microchannel heat sink (straight channel design) in order to reduce the substrate temperature is not an effective method because it reduces the effective energy consumption. So in this paper, Rib-groove microchannel heat sink design is proposed in order to the minimize the substrate temperature with effective energy consumption. In the present study, the effect of triangular groove geometry parameter was analysed numerically for the Re number ranging between 100 to 800. The result showed that, Rib-groove microchannel heat sink (TC-RR MCHS) with triangular cavities pitch location of 140 µm (CV3) obtained the lowest average substrate temperature, $T_{b,ave}$ for all Re number. Besides that, the TC-RR MCHS with CV3 design only required 1.82 mW of pumping power while the straight microchannel heat sink (CR MCHS) required 14.94 mW of pumping power in order to achieve the lowest average substrate temperature in the CR MCHS. Means that, the proposed design saved the energy consumption up to 87.8%.

Keywords:
Rib-groove microchannel heat sink; substrate temperature; pumping power consumption; energy consumption

1. Introduction

Nowadays, fast development in electronic industry witnesses many advanced technologies with unpredicted increment power density in their system especially in MEMS devices. As consequence,

* *Corresponding author.*
E-mail address: azwadi@utm.my (Nor Azwadi Che Sidik)

high heat flux is generated by those devices and thus reduces the performance of its system. Generally, the reliability of those devices might be reduced up to 50% of the original value if the temperature of the devices increase 10^o sharply [1]. So, in order to maintain the device performance, high performance cooling techniques are required to improve its cooling system. Microchannel heat sink is one of the cooling techniques that can meet the current cooling demand whereby the optimum junction temperature for electronic device should be controlled below than 358.15 K [2].

The first concept of microchannel heat sink was pioneered by Tuckerman and Pease [3] in 1981 from Stanford University, who performed the investigation of microchannel performance through experiment. In their study, the microchannel was fabricated by silicon and water was utilized as a fluid transportation. They demonstrated that, the straight channel microchannel heat can remove heat flux up to 790 W/m^2 with the temperature difference between the substrate and water inlet of 71^{o}C. However, high mass flowrate was required to remove the heat flux due to thickened boundary layer in laminar flow. They suggested to used fin structure as a flow disruption in order to increase the thermal performance in the straight channel microchannel heat sink. Since then, many enhancement techniques were proposed in the open literature and can be grouped in two methods, active and passive method. Many scholars are more attracted to the passive method attributes to no additional spacing in cooling system, no external energy is required to improve heat transfer performance and no moving part whereby in contrast to air.

In recent years, many invention and innovation focus on single-layered microchannel heat sink [4-12], multi-layered microchannel heat sink [13, 14] and multi-layered microchannel heat with alternate structure [15]. Besides that, some former researchers are also interested on the utilization of nanofluid in microchannel heat sink application as reported in a comprehensive review paper published by Japar *et al.,* [16]. But, in current study, the investigation of passive method focused on single-layered microchannel heat sink. Flow disruption is one of the effective passive method that can intensively changes the flow structure of laminar by providing “blocking effect” either at the sidewalls or at the centre portion of channel. The “blocking effect” increases the degree of flow mixing between cold and hot water which contributes to the enhancement of heat transfer performance. In 2009, Hong and Cheng tried to explore the potential of offset strip-fin in microchannel design. They proved that, the existing of fins gradually increased the heat transfer performance in microchannel heat sink with excessive pressure drop penalty [17]. High degree of flow fixing also can be obtained by secondary channel geometry without any significant effect on pressure drop penalty. Lee *et al.,* [18] adopted this geometry in their novel microchannel heat sink. The secondary channel was created by copper oblique fins in the microchannel heat sink. They demonstrated that, heat transfer enhancement can be obtained by the secondary channel minimal pressure drop. Next two years, Lee and his team [19] published their other comprehensive study by optimizing the oblique fins geometry parameter which extended form their previous work [18]. The optimization outcome revealed that oblique fin with smaller angle and smaller fin pitch contributed to the higher heat transfer performance enhancement. However, from the view point of thermal management, this method is not very effective as a flow disruption method.

Above studies clearly show that, single passive method such as flow disruption can provide high heat transfer rate in an enhanced microchannel sinks. However, pressure drop issue becomes the bottleneck of further development of single passive method a thermal microchannel heat sink. Nowadays, many single-layered microchannel heat sinks are designed by more than one single passive method which called as hybrid passive method. In hybrid passive method, the balance between strength and weakness of single passive method are considered in microchannel design in order to obtain high heat transfer rate with minimal pressure drop. In 2013, Gong *et al.,* [20] analysed the performance of microchannel that structured by dimple geometry and wavy shape. In their

design, the effect of dimple number in wavy channel has been study numerically. The highest Performance Factor of 1.42 was achieved at Re number of 200. They revealed that the presence of the dimple structure in wavy channel enhanced the heat transfer performance and not apparently increase the flow resistance. Li *et al.,* [21] presented a numerical study to investigate the effect of ribs and cavities on fluid flow and heat transfer characteristic. The analysis revealed that combined effect of interruption, redevelopment of thermal boundary layer, the intensified mainstream disturbance and the chaotic mixing between hot and cold water contributed to enhancement of heat transfer performance. The Performance Factor of this design is higher than the dimple-wavy microchannel heat sink. The highest Performance Factor of this design was 1.62 and achieved at Re number of 500.

The hybrid designs presented in above literatures show that, the remarkable optimum overall performance of the enhanced microchannel heat sink can be obtained at high Re number which contributes to the high pumping power consumption. However, to the best of author's knowledge, only few studies focused on this characteristic. So in the present study, we extended Li *et al.,* [21]'work in order to enhance the heat transfer performance that contributes to the Performance Factor augmentation with effective pumping power consumption compared to conventional design microchannel heat sink (CR MCHS). In this study, three different shapes (CV1, CV2 and CV3) of triangular groove geometry in a hybrid design (TC-RR MCHS) are analysed numerically for the Re number ranging between 100 to 800. The shape of triangular groove geometry depends on the location of triangular groove corner along flow direction. Those three shapes performances are measured based on the average substrate temperature and pumping power consumption.

2. Geometry parameter of microchannel heat sink

The TC-RR MCHS is fabricated by copper and consist of ten microchannels on the heat sink. All the microchannel has a same geometry structure. In the current study, only one symmetrical part of microchannel was analysed due to computational cost and time. The single wall microchannel of TC-RR MCHS as shown in Figure 1(a) was selected as the symmetrical part and used in all analyses. Figure 1(b) illustrates the geometry parameter of the single wall microchannel that involves in this study. The details of all the parameter is showed in Table 1. The groove length is constant for all analyses. Only L1 and L2 parameters change based on shape design of CV1, CV2 and CV3.

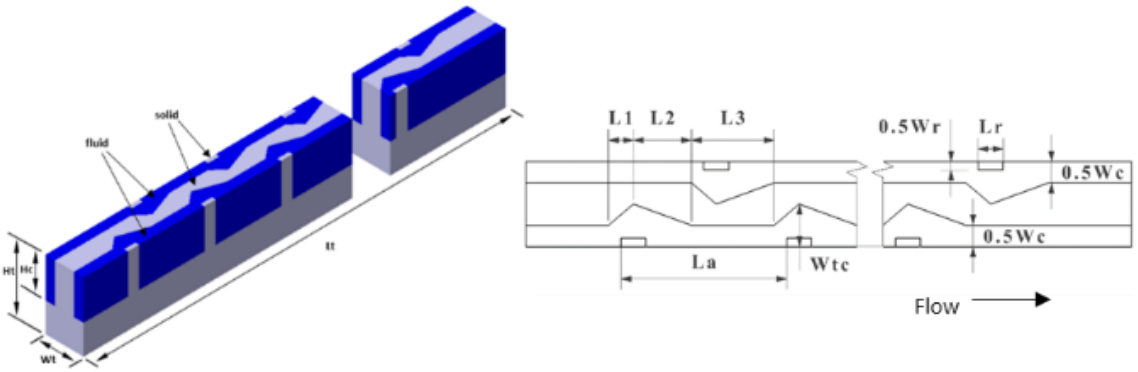

(a) (b)

Fig. 1. TC-RR MCHS (a) One symmetrical part (b) Geometry parameter

Table 1
Geometry parameters of TC-RR MCHS

Parameter	Value
Lt	10,000 µm
Wt	200 µm
Ht	350 µm
Hc	200 µm
Wc	100 µm
Lr	60 µm
Wr	30 µm
La	400 µm
L1 & L2 (Three different shape)	**CV1:** - L1: 60 µm - L2: 140 µm **CV2:** - L1: 100 µm - L2: 100 µm **CV3:** - L1: 140 µm - L2: 60 µm
L3	200 µm
Wtc	112 µm

The shape of those designs are illustrated in Figure 2. The figure shows that, the shape of triangular groove changes with L1 and L2 parameters. The rib geometry is fixed at original location. Figure 2 is a top view of a triangular groove.

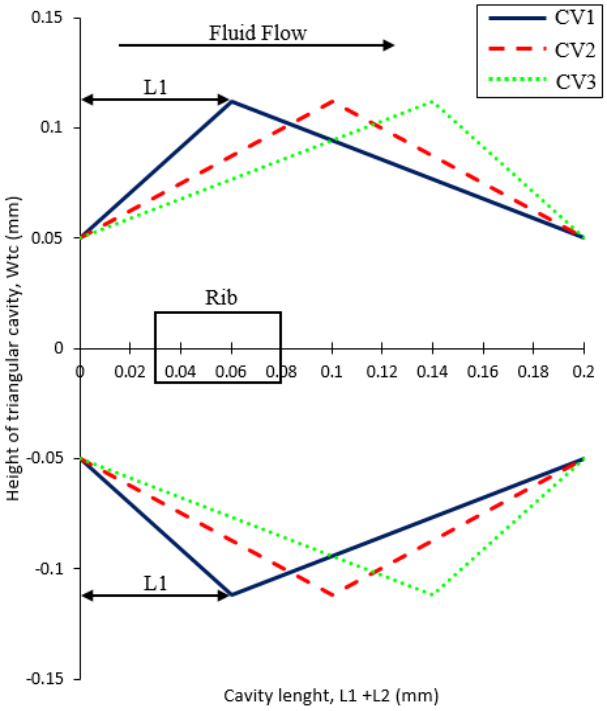

Fig. 2. Triangular cavities with three different shape

3. Numerical method approach

A Computational Fluid Dynamic (CFD) software such as ANSYS FLUENT 17.0 is used to solve the governing equations in a three dimensional designs according to the following assumptions.

- In the present study, fluid flow in all simulated geometry designs are continuum due to Knudsen number, (*Kn*) for the fluid flow is less than (10^{-3}) [22].
- For the continuum flow, Navier-Stokes equation and non-slip boundary condition are applicable
- Fluid is Newtonian and incompressible
- Due to microscopic size of channel and to prevent a high pressure drop, laminar flow is applied for all geometry.
- Fluid flow and heat transfer are simulated in steady-state.
- Constant thermophysical properties.
- Viscous dissipation is neglected due to the highest pressure drop in present study is less than 1 MPa with considering the first law of thermodynamics.
- Gravitational force and radiation heat transfer are neglected.

3.1 Governing equations

Based on the assumptions that made in the present study, governing equation for conservation of mass, momentum and energy equations can be written as:

Continuity equation:

$$\frac{\partial u}{\partial x}+\frac{\partial v}{\partial y}+\frac{\partial w}{\partial z}=0 \tag{1}$$

Where *u, v* and *w* are the velocity components in *x*, *y* and *z*-directions respectively.

Momentum equation:

$$u\frac{\partial u}{\partial x}+v\frac{\partial u}{\partial y}+w\frac{\partial u}{\partial z}=-\frac{1}{\rho_f}\frac{\partial p}{\partial x}+\frac{\mu_f}{\rho_f}\left(\frac{\partial^2 u}{\partial x^2}+\frac{\partial^2 u}{\partial y^2}+\frac{\partial^2 u}{\partial z^2}\right) \tag{2}$$

$$u\frac{\partial v}{\partial x}+v\frac{\partial v}{\partial y}+w\frac{\partial v}{\partial z}=-\frac{1}{\rho_f}\frac{\partial p}{\partial y}+\frac{\mu_f}{\rho_f}\left(\frac{\partial^2 v}{\partial x^2}+\frac{\partial^2 v}{\partial y^2}+\frac{\partial^2 v}{\partial z^2}\right) \tag{3}$$

$$u\frac{\partial w}{\partial x}+v\frac{\partial w}{\partial y}+w\frac{\partial w}{\partial z}=-\frac{1}{\rho_f}\frac{\partial p}{\partial z}+\frac{\mu_f}{\rho_f}\left(\frac{\partial^2 w}{\partial x^2}+\frac{\partial^2 w}{\partial y^2}+\frac{\partial^2 w}{\partial z^2}\right) \tag{4}$$

Where ρ_f and μ_f are the density and dynamic viscosity of the working fluid(water), respectively, and *p* is the fluid(water) pressure.

There are two energy equations that related to the present study, namely, energy equation for fluid region (Eq. (5)) and energy equation for solid region (Eq. (6)):

$$u\frac{\partial T_f}{\partial x}+v\frac{\partial T_f}{\partial y}+w\frac{\partial T_f}{\partial z}=\frac{k_f}{\rho_f c_{Pf}}\left(\frac{\partial^2 T_f}{\partial x^2}+\frac{\partial^2 T_f}{\partial y^2}+\frac{\partial^2 T_f}{\partial z^2}\right) \quad (5)$$

$$0=k_s\left(\frac{\partial^2 T_s}{\partial x^2}+\frac{\partial^2 T_s}{\partial y^2}+\frac{\partial^2 T_s}{\partial z^2}\right) \quad (6)$$

Where T_f, T_s, k_f, k_s and Cp_f are the fluid's temperature, solid's temperature, fluid thermal conductivity, solid thermal conductivity and fluid specific heat, respectively.

3.2 Boundary Condition

Boundary condition is a condition for hydrodynamic and thermal that we applied on the simulated geometries in the present study. Uniform velocity with the temperature of 300 K is applied on the inlet channel for all cases. While at the outlet, we set as atmospheric pressure. A uniform heat flux of 100W/cm^2 is applied on the substrate of the heat sink. At the fluid-solid interface, no-slip and no penetration are assumed. Table 2 shows the details for other boundary conditions.

Table 2
Boundary condition

Boundary	Location	Condition
Hydrodynamic	At the fluid-solid interface	No-slip and no penetration $u=v=w=0$ $-k_s\left(\frac{\partial T_s}{\partial n}\right)=-k_f\left(\frac{\partial T_f}{\partial n}\right)$ where n is the coordinate normal to the wall
	At inlet, $x=0$	$u_f=u_{in}$ $v=w=0$
	At outlet, $x=L_t=10mm$	$p_f=p_{out}=1atm$
Thermal	At inlet, $x=0$	$T_f=T_{in}=300\,K$ (for water) $-k_s\left(\frac{\partial T_s}{\partial x}\right)=0$ (for solid)
	At outlet, $x=L_t=10mm$	$-k_f\left(\frac{\partial T_f}{\partial x}\right)=0$ (for water) $-k_s\left(\frac{\partial T_s}{\partial x}\right)=0$ (for solid)
	At top wall, $z=Ht=0.35mm$	$u=v=w=0$ $-k_s\left(\frac{\partial T_s}{\partial z}\right)=0$
	At bottom wall, $z=0$	$-k_s\left(\frac{\partial T_s}{\partial z}\right)=q=100W/cm^2$
	At side wall, $y=0$	$\frac{\partial}{\partial y}=0$ (symmetry)
	At side wall, $y=Wt=0.2mm$	$\frac{\partial}{\partial y}=0$ (symmetry)

3.3 Grid independency test and CFD simulation

Mesh quality is very important to the convergence of numerical solution and numerical computation stability. In this paper, ANSYS is used to generate hexahedral meshing structure which can provide a faster solution time. Figure 3 illustrates the hexahedral mesh structure in TC-RR MCHS design. Finite volume method is utilized to discretize the governing equation. The SIMPLE algorithm was adopted to accomplish the pressure-velocity coupling. Furthermore, convergence criteria are set to be less than 10^{-6} for continuity and less than 10^{-9} for energy.

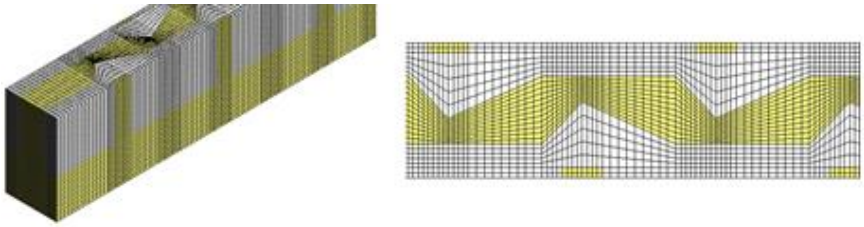

(a) (b)

Fig. 3. Computational grid of TC-RR MCHS (a) Isometric view (b) Top view at x-z plane

Grid independency test is a process to find the optimum mesh structure that can be adopted in TC-RR MCHS design, so that the design can produce an accurate result with the lower time cost. Besides that, the test was conducted in order to ensure the simulation results are not affected by the grid size. The process is started with a fine mesh structure to a coarse mesh structure in a base design (CR MCHS). In the present study, the total number of element or grid for the finest mesh is 0.5 million for Reynolds number of 800. With the same Reynolds number, the number of element is reduced up to 0.15 million. By considering Nusselt number and pressure drop for each element number, the optimum mesh structure is obtained by calculating the relative error using following equation:

$$e\% = \left| \frac{J_2 - J_1}{J_1} \right| \times 100 \tag{7}$$

Where J_1 represents the value of Nusselt number and pressure drop for the finest mesh structure while J_2 represents the value of Nusselt number and pressure drop for the coarser mesh. Based on the relative error presented in Table 3 for each element number, it clearly observed that element number of 0.3 million ($e\% \leq 0.1$) has a reasonable accuracy compared with other element numbers. Consequently, the number element of 0.3 million is adopted for all cases in current study.

Table 3
Grid independence test

Grid number (X10^5)	Nu	*e%*	Pressure drop (Pa)	*e%*
5.0	9.29	-	124031.57	-
4.0	9.29	0	123987.20	0.036
3.5	9.29	0	123956.07	0.061
3.0	9.29	0	123915.92	0.093
2.5	9.29	0	123866.06	0.133
2.0	9.29	0	123816.87	0.173
1.5	9.29	0	123788.96	0.196

3.4 Data reduction

This section presents the relevant expressions that used to calculate the characteristics of heat transfer and fluid flow in microchannel heat sink.

The Reynolds number (Re) is expressed as follow:

$$\mathrm{Re} = \frac{\rho u_m D_h}{\mu} \tag{8}$$

Where D_h represents the hydraulic diameter and it is calculated as follow:

$$D_h = \frac{2H_c W_c}{H_c + W_c} \tag{9}$$

The average apparent friction factor and pumping power are given by:

$$f_{app,ave} = \frac{2D_h \Delta P}{Lt \rho u_m^2} \tag{10}$$

$$P_p = \dot{V} \Delta P \tag{11}$$

Where L_t and ΔP are the total length of microchannel and pressure drop across microchannel respectively. The average heat transfer coefficient and the average Nusselt number are given by:

$$h_{ave} = \frac{q_w A_{film}}{A_{con.}(T_{W,ave} - T_{f,ave})} \tag{12}$$

$$Nu_{ave} = \frac{h_{ave} D_h}{k_f} \tag{13}$$

Where q_w, A_{film}, A_{cond}, $T_{w,ave}$ *and* $T_{f,ave}$ are the heat flux per unit area, heated area, convection heat transfer area, average temperature of wall and average temperature of fluid, respectively.

4. Result and discussion

In order to verify the accuracy of the simulation model approach, data that obtained from simulation analysis, namely, friction factor and pressure drop for the base design (CR MCHS) are validated with previous correlations developed by former researchers. The friction factor is validated with Shah & London correlation [23]:

$$f_{app,ave}\,\mathrm{Re} = \left[\left(\frac{3.2}{Lt/\mathrm{Re}\,D_h}\right)^2 + (Po)^2\right]^{\frac{1}{2}} \tag{14}$$

Poiseuille number (*Po*):

$$P_O = 96[1-1.3553(AR)+1.946(AR)^2-1.7012(AR)^3+0.9564(AR)^4-0.2537(AR)^5] \quad (15)$$

Pressure drop is validated with Steinke and Kandlikar [24]:

$$\Delta p = \frac{2(f\,\mathrm{Re})\mu_f u_m Lt}{D_h^2} + \frac{K\rho_f u_m^2}{2} \quad (16)$$

$$f\,\mathrm{Re} = 24\left(1-1.3553\alpha_c+1.9467\alpha_c^2+1.7012\alpha_c^3+0.9564\alpha_c^4+0.2537\alpha_c^5\right) \quad (17)$$

$$K = 0.6797+1.2197\alpha_c+3.3089\alpha_c^2-9.5921\alpha_c^3+8.9089\alpha_c^4-2.9959\alpha_c^5 \quad (18)$$

Where α_c is channel aspect ratio of width to height and K is Hagenbach's factor.

Validation of the simulation model with the previous correlations are illustrated in Figure 4. It clearly shows the simulation result has a good agreement with both correlations. This agreement indicates that the simulation model approach can be referred to predict the fluid flow and heat transfer characteristic in present study for all designs.

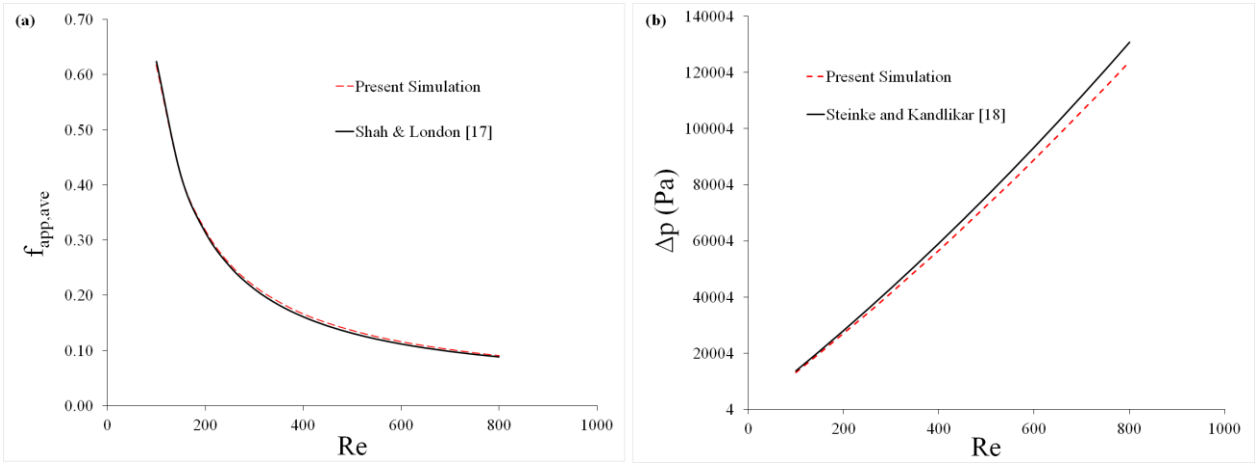

Fig. 4. Model validation (a) Friction factor according to Shah & London [17] (b) Pressure drop according to Steinke & Kandlikar [18].

As mentioned in above background study, the substrate temperature of microchannel heat sink is very important because it directly attaches to electronic components. So in this section, the performance of each design is evaluated based on the substrate temperature of microchannel heat sink. Figure 5 illustrates the substrate temperature of base design (CR MCHS) and enhanced designs (CV1, CV2 and CV3) from the bottom view with unshaded surface at Re number of 350. The figure shows CR MCHS obtain the highest substrate temperature distribution compared to the enhanced designs. The highest substrate temperature, $T_{b,\,max}$ of the CR MCHS is 326.22 K. It happens due to the boundary layer in laminar region is so thick and thus increases the thermal resistance in the fluid region. For the enhanced designs, TC-RR MCHS with CV3 design shows the lowest substrate temperature distribution than CV1 and CV2 designs. It is proven by the temperature distribution at the channel length, Lt of 5.1 mm. At that location, the substrate temperature distribution of CV3 is around 309.5 K compared to CV1 and CV2 with substrate temperature distribution of 310 K. Besides that, CV3 design reduces the maximum substrate temperate of CR MCHS by 3.8% compared to CV1 and CV2 that only by 3.6% for both designs. Means that, triangular groove geometry parameters have a significant effect on thermal performance.

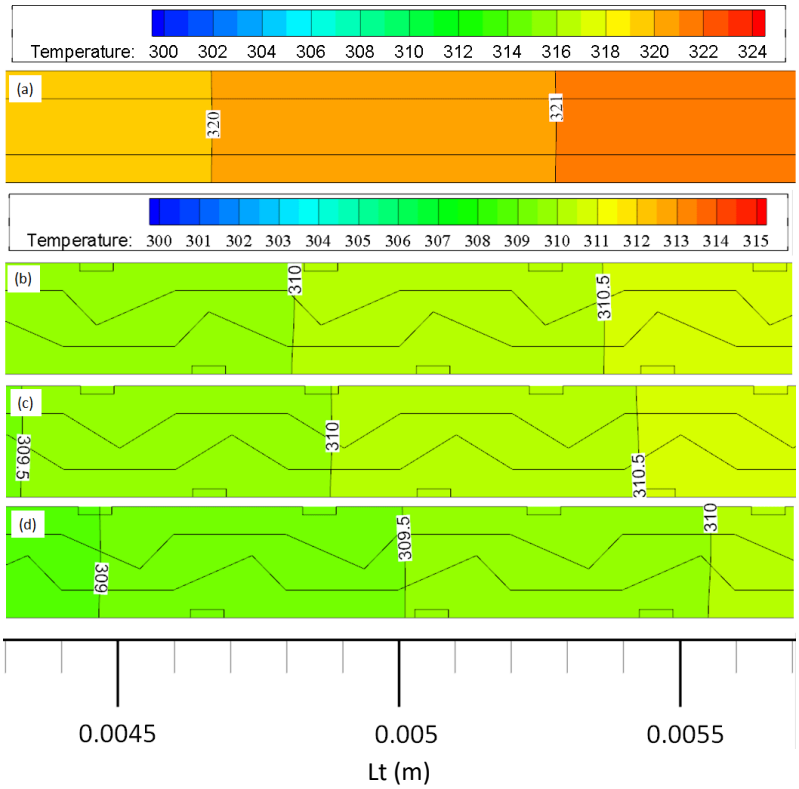

Fig. 5. Substrate temperature of microchannel sink from the bottom view with unshaded surface at Re=350 (a) CR MCHS with $T_{b,max}$=326.22 K (b) CV1 design with $T_{b,max}$=314.60 K (c) CV2 design with $T_{b,max}$=314.47 K (d) CV3 design with $T_{b,max}$=313.81 K

Figure 6 demonstrates the average substrate temperature, $T_{b,ave}$ of CR MCHS and TC- RR MCHS with different triangular groove shape (CV1, CV2 and CV3) for Re number of 100 to 800. The figure shows that, when the Re number increases, the average substrate temperature, $T_{b,ave}$ of all designs decreases sharply until a certain Re number and then decreases slowly until Re = 800. As expected, CR MCHS obtain the highest average substrate temperature, $T_{b,ave}$ compared to the enhanced designs due to thermal resistance created by laminar region. For enhanced designs, the average substrate temperature, $T_{b,ave}$ of CV1, CV2 and CV3 are quite similar at the lower Re number. But then, when the Re number increases further, the average substrate temperature, $T_{b,ave}$ of CV3, decreases significantly compared to CV1 and CV2 designs. However, from the viewpoint of energy saving, achieves high thermal performance with minimal pumping power consumption is good for enhanced microchannel heat sink in order to replace the CR MCHS as a cooling device.

To achieve the cooling requirement with effective energy consumption, the analysis between the average substrate temperature, $T_{b,ave}$ and pumping power consumption, P is conducted as shown in Figure 7. The figure presented that, when the mass flowrate of fluid increased, the average substrate temperature decreased while the pumping power consumption increased. As illustrated in the figure, CR MCHS requires 12.04×10^{-5} kg/s mass flowrate to achieve the lowest average substrate temperature of 314.1 K which consumes 14.94 mWatt pumping power. However, TC-RR MCHS with CV3 design only requires 3.01×10^{-5} kg/s mass flowrate to achieve the average substrate temperature of 314.1 K same as the lowest average substrate temperature of CR MCHS. Means that, the TC-RR MCHS with CV3 design saves the energy consumption up to 87.8%, because only consumes 1.82 mWatt pumping power in order to pump the mass flowrate of 3.01×10^{-5} kg/s.

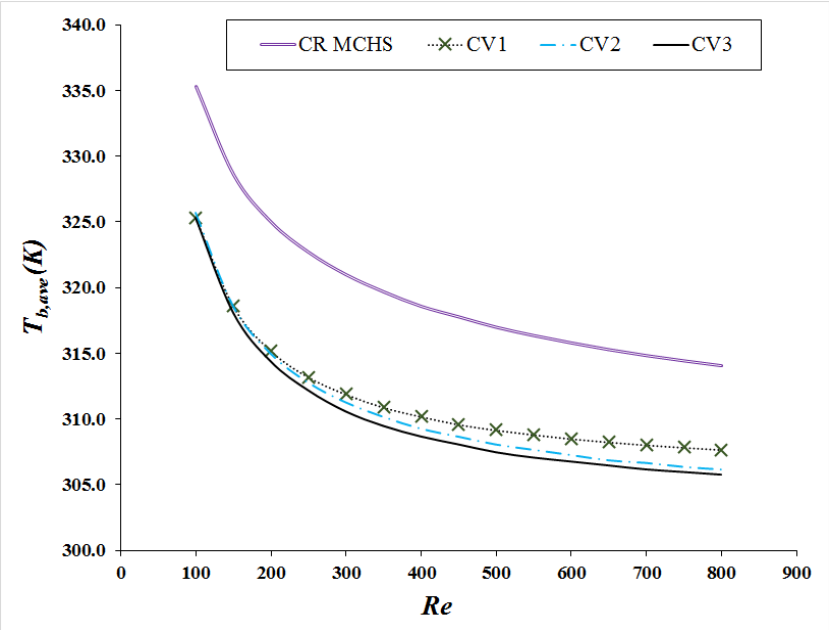

Fig. 6. Average substrate temperature, $T_{b,ave}$ of CR MCHS and enhanced MCHS

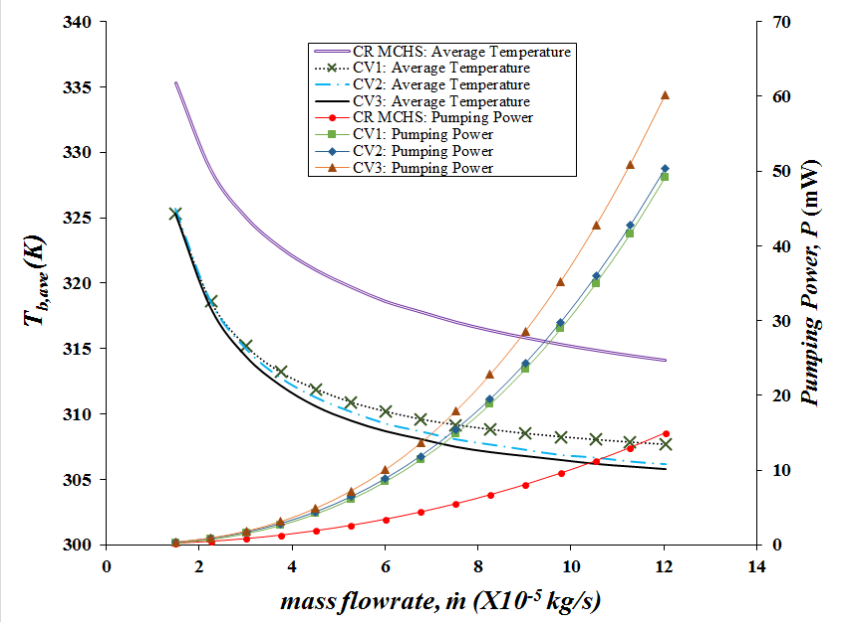

Fig. 7. Average substrate temperature, $T_{b,ave}$ and pumping power of CR MCHS and enhanced MCHS

5. Conclusion

In this study, TC-RR MCHS with three different triangular grooves (CV1, CV2 and CV3) were investigated numerically in order to optimize the heat transfer performance with minimal pressure drop compared to the base design or conventional microchannel heat sink (CR MCHS) for Re number of 100 to 800. The study showed that TC-RR MCHS with CV3 design obtained the lowest average substrate temperature than CV1 and CV2 design for all Re number and saved energy consumption up to 87.8% compared to the conventional design (CR MCHS). Means that, this design can be used in an application which not requires a high energy consumption for their cooling system.

Acknowledgment and Funding

Authors wish to thanks Universiti Teknologi Malaysia for supporting this research activity by the Takasago grant [R.K130000.7343.4B365].

Reference

[1] Li, Yanlong, Fengli Zhang, Bengt Sunden and Gongnan Xie. "Laminar thermal performance of microchannel heat sinks with constructal vertical Y-shaped bifurcation plates." *Applied Thermal Engineering* 73, no. 1 (2014): 185-195.

[2] Yan, Yunfei, Hongyu Yan, Siyou Yin, Li Zhang and Lixian Li. "Single/multi-objective optimizations on hydraulic and thermal management in micro-channel heat sink with bionic Y-shaped fractal network by genetic algorithm coupled with numerical simulation." *International Journal of Heat and Mass Transfer* 129 (2019): 468-479.

[3] Tuckerman, David B and Roger Fabian W Pease. "High-performance heat sinking for VLSI." *IEEE Electron device letters* 2, no. 5 (1981): 126-129.

[4] Japar, Wan Mohd Arif Aziz, Nor Azwadi Che Sidik and Shabudin Mat. "A comprehensive study on heat transfer enhancement in microchannel heat sink with secondary channel." *International Communications in Heat and Mass Transfer* 99 (2018): 62-81.

[5] Japar, Wmaa and N. A. C. Sidik. *The effectiveness of secondary channel on the performance of hybrid microchannel heat sink at low pumping power*. in *Materials Science and Engineering*. 2019. IOP Publishing.

[6] Beng, Soo Weng and Wan Mohd Arif Aziz Japar. "Numerical analysis of heat and fluid flow in microchannel heat sink with triangular cavities." *Journal of Advanced research in fluid mechanics and thermal sciences* 34 (2017): 1-8.

[7] S. B. Abubakar, N. A. Che Sidik and A.S. Ahmad. "The use of Fe3O4-H2O4 Nanofluid for Heat Transfer Enhancement in Rectangular Microchannel Heatsink." *Journal of Advanced Research in Materials Science* 23 (2016): 15-24.

[8] Thillai Mugilan, Nor Azwadi Che Sidik, Wan Mohd Arif Aziz Japar. "The Use of Smart Material of Nanofluid for Heat Transfer Enhancement in Microtube with Helically Spiral Rib and Groove." *Journal of Advanced Research in Materials Science* 32 (2017): 1-12.

[9] S. Zainal, C. Tan, C. J. Sian and T. J. Siang. "ANSYS simulation for Ag/HEG Hybrid Nanofluid in Turbulent Circular Pipe." *Journal of Advanced Research in Applied Mechanics* 23 (2016): 20-35.

[10] A. A. Razali and A. Sadikin. "CFD Simulation Study on Pressure Drop and Velocity across Single Flow Microchannel Heat Sink." *Journal of Advanced Research Design* 8 (2015): 12-21.

[11] Saidu Bello AbuBakar, Nor Azwadi Che Sidik, Hong Wei Xian. "Numerical Prediction of Laminar Nanofluid Flow in Rectangular Microchannel." *Journal of Advanced Research Design* 50 (2018): 1-17.

[12] Wan Mohd. Arif Aziz Japar, Nor Azwadi Che Sidik, M'hamed Beriache. "Hydrothermal Performance in a New Designed Hybrid Microchannel Heat Sink with Optimum Secondary Channel Geometry Parameter: Numerical and Experimental Studies." *Journal of Advanced Research Design* 54 (2019): 13-27.

[13] Chamoli, Sunil, Ruixin Lu, Hao Chen, Yongpan Cheng and Peng Yu. "Numerical optimization of design parameters for a modified double-layer microchannel heat sink." *International Journal of Heat and Mass Transfer* 138 (2019): 373-389.

[14] Zuo, J. W., K. C. Wong and H. K. Ng. "The thermal performance of three-layered microchannel heat sink with tapered channel profile." *Journal of Advanced Research in Fluid Mechanics and Thermal Sciences* 56, no. 1 (2019): 147-156.

[15] Shen, Han, Gongnan Xie and Chi-Chuan Wang. "Heat transfer and thermodynamic analysis by introducing multiple alternation structures into double-layer microchannel heat sinks." *International Journal of Thermal Sciences* 145 (2019): 105975.

[16] Japar, Wan Mohd Arif Aziz, Nor Azwadi Che Sidik, Siti Rahmah Aid, Yutaka Asako and Tan Lit Ken. "A Comprehensive Review on Numerical and Experimental Study of Nanofluid Performance in Microchannel Heatsink (MCHS)." *Journal of Advanced Research in Fluid Mechanics and Thermal Sciences* 45, no. 1 (2018): 165 – 176.

[17] Hong, Fangjun and Ping Cheng. "Three dimensional numerical analyses and optimization of offset strip-fin microchannel heat sinks." *International Communications in Heat and Mass Transfer* 36, no. 7 (2009): 651-656.

[18] Lee, YJ, PS Lee and SK Chou. "Enhanced thermal transport in microchannel using oblique fins." *Journal of Heat Transfer* 134, no. 10 (2012): 101901.

[19] Lee, Yong Jiun, Pawan K Singh and Poh Seng Lee. "Fluid flow and heat transfer investigations on enhanced microchannel heat sink using oblique fins with parametric study." *International Journal of Heat and Mass Transfer* 81 (2015): 325-336.

[20] Gong, Liang and Bo Wei. *The Characteristics of Fluid Flow and Heat Transfer in Wavy, Dimple and Wavy-Dimple Microchannels*. in *Applied Mechanics and Materials*. 2013. Trans Tech Publ.

[21] Li, YF, GD Xia, DD Ma, YT Jia and J Wang. "Characteristics of laminar flow and heat transfer in microchannel heat sink with triangular cavities and rectangular ribs." *International Journal of Heat and Mass Transfer* 98 (2016): 17-28.
[22] Service, Robert F. "Coming soon: the pocket DNA sequencer." *Science (New York, NY)* 282, no. 5388 (1998): 399.
[23] Shah, Ramesh K and Alexander Louis London, *Laminar flow forced convection heat transfer and flow friction in straight and curved ducts-A summary of analytical solutions*. 1971, Stanford Univ CA Dept of Mechanical Engineering.
[24] Steinke, Mark E and Satish G Kandlikar. "Single-phase liquid friction factors in microchannels." *International Journal of Thermal Sciences* 11, no. 45 (2006): 1073-1083.